热力循环

文章编号: 1001 - 2060(2011) 05 - 0533 - 05

辐射传热定律下外燃机最大输出功优化

马　康, 陈林根, 孙丰瑞
(海军工程大学 研究生院, 湖北 武汉 430033)

摘　要: 以活塞式外燃机为研究对象, 考虑工质与外热槽间传热服从辐射传热定律 [$q \propto \Delta(T^4)$], 以循环输出功最大为优化目标进行了优化。给出了辐射传热定律下的数值算例, 并与牛顿传热定律下的结果进行了比较。结果表明, 热导率增加, 最优完全循环和半循环的输出功和效率均减小, 与完全循环相比, 最优半循环的压缩比、输出功和效率较大; 结果还说明虽然两种传热定律下最优完全循环和最优半循环的欧拉-拉格朗日($E-L$)弧部分的工质体积随时间的变化曲线均类似于正弦曲线, 并且均由 3 部分组成, 但不同传热定律下工质体积随时间的变化曲线是不相同的。

关　键　词: 有限时间热力学; 辐射传热定律; 最大输出功; 外燃机

中图分类号: TK12　　文献标识码: A

引　言

有限时间热力学是研究各种热力过程和循环的有力工具[1~3], 求出给定最优目标时与其最佳值对应的最优热力过程, 即最优构型问题, 是有限时间热力学主要研究的问题之一。解决最优构型问题可以采用两种求解方法: 欧拉—拉格朗日方程和最优控制理论。最优构型问题的实质是求出对应于某种要求的性能目标达到最大值时动态系统(受控对象)从初态转移到某种要求的末态的最优路径, 同时最优构型一旦求出, 所有其它热力学量都可以从中得到。Band 等人研究了牛顿传热条件下活塞式加热气缸膨胀功最大时的最优路径[4~6], 得出了其最优路径包括两个瞬时绝热分支和一个最大膨胀功输出分支(欧拉 - 拉格朗日弧($E-L$))等 3 个分支[4~5], 并将结果应用到外燃机运行过程优化中[6]。Salamon 和 Aizenbud 等人进一步考虑了活塞式加热气缸最大功率输出时的最优路径[7~8], 以及给定输出功率时的最大输出功的最优构型。Aizenbud 等人将文献[5]的结果进一步应用到内燃机运行过程优化中[9]。实际传热定律并不是总是服从牛顿传热定律的, 传热定律不仅影响给定热力过程的性能, 而且影响给定优化目标时的最优热力过程。陈林根等人研究了线性唯象[$q \propto \Delta(T^{-1})$]和对流辐射复合[$q \propto \Delta(T) + \Delta(T^4)$]传热定律下的活塞式气缸中加热气体的最优膨胀规律[10~11]。宋汉江等人利用泰勒公式展开法得到了广义辐射传热定律[$q \propto \Delta(T^n)$]下膨胀过程时间较短(如文献[12]给出的 $t = 0.05$ s)时 $E-L$ 弧的近似解析解[12]。马康等人利用消元法重新研究了广义辐射传热定律下最优膨胀问题[13], 得到了平方传热定律[$q \propto \Delta(T^2)$]和立方传热定律[$q \propto \Delta(T^3)$]下气体最优膨胀的准确解析解。宋汉江和陈林根等人研究线性唯象传热定律下外燃机和内燃机运行过程的优化问题[14~15]。

本研究是在文献[5~6, 13~14]的基础上, 以活塞式外燃机(这里所考虑的外燃机是完全循环, 即温度和容积在压缩和动力冲程中是周期性变化的, 不考虑其它冲程)为研究对象, 考虑工质与外热槽间传热服从辐射传热定律[$q \propto \Delta(T^4)$], 以循环输出功最大为优化目标, 对外燃机运行过程的优化进行研究。给出辐射传热定律时的数值算例, 并与牛顿传热定律下的结果进行比较。在活塞式外燃机模型中引入辐射传热定律, 丰富了有限时间热力学理论, 使其更加系统和完善。

1　$E-L$ 弧

设活塞式气缸中含有理想气体, 伴有给定的泵入热流率 $f(t)$, 气缸与外热槽的热交换服从辐射传热定律[$q \propto \Delta(T^4)$], q 为穿过气缸壁的热流率, U 为热导率, T 和 T_{ex} 分别为工质和热槽的温度, 理想

收稿日期: 2010 - 03 - 04;　修订日期: 2010 - 09 - 01
基金项目: 国家自然科学基金资助项目(10905093), 教育部新世纪优秀人才支持计划基金资助项目(NCET - 04 - 1006); 全国优秀博士论文作者专项资金资助项目(200136)
作者简介: 马　康(1981 -), 男, 湖北十堰人, 海军工程大学博士研究生.

气体的初始内能 $E(0)$、体积 $V(0)$、和终态体积 V_m 为已知。根据文献[6,13],假设气缸壁热传导速度非常快,气缸的每一部分均在加热,从而可以忽略活塞位置对热导率 U 的影响。因此,认为气缸壁的热导率在整个膨胀过程中为常数。

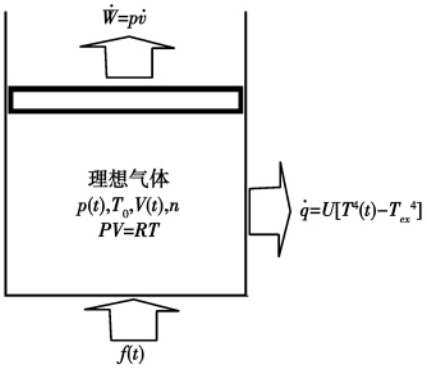

图 1 活塞式气缸示意图

Fig. 1 Schematic drawing of a plunger type cylinder

活塞式外燃机气缸如图 1 所示,忽略气体和活塞的惯性影响,不计活塞运动的摩擦效应,则由热力学第一定律得:

$$\dot{E}(t)=f(t)-\dot{W}(t)-U[T^4(t)-T_{ex}^4] \tag{1}$$

式中: $E(t)$—气体内能; $W(t)$—功,各量上的小点表示该量随时间变化的速率。

优化的目标是使加热工质在膨胀过程中的输出功最大。根据文献[13]的结论,活塞式气缸最大膨胀功时的最优运动由 3 部分组成:

(1) 在 $t=0$ 时刻从 $V(0)$ 到 $V'(0)$ 的绝热过程:

$$E'(0)=E(0)[V'(0)/V(0)]^{-R/C_V} \tag{2}$$

式中: $V'(0)$ 和 $E'(0)$—初始绝热过程的终点。

(2) 在 $t=0$ 至 $t=t_m$ 之间的弧。中间的 $E-L$ 弧部分由下面两个式子给出[13]:

$$E^5(t)-\frac{3UE^5(t_i)}{3UE^4(t_i)+C_V^4F(t_i)}E^4(t)-\frac{C_V^4E^5(t_i)}{3UE^4(t_i)+C_V^4F(t_i)}F(t)=0 \tag{3}$$

$$V(t)=V'(0)\left[\frac{E(t)}{E'(0)}\right]^{C_V/R}\exp\left\{\frac{C_V}{R}\times\int_0^t\frac{F(t)-U[E(T)/C_V]^4}{E(t)}\mathrm{d}t\right\} \tag{4}$$

式中: C_V—摩尔热容; R—理想气体常数; t_m—循环周期, $F(t)=f(t)+UT_{ex}^4$。

由于式(3)是高次方程,无法直接求解得到 $E(t)$ 的解析式,因此只能通过数值求解的方法得到 $E-L$ 弧。

(3) 在 $t=t_m$ 时刻到给定最终容积 V_m 的绝热过程:

$$E_m=E(t_m)[V_m/V(t_m)]^{-R/C_V} \tag{5}$$

式中: $E(t_m)$、$V(t_m)$—由式(3)和式(4)求出。

2 外燃机运行过程优化中的应用

文献[13]研究了辐射传热定律下活塞式气缸输出功最大时的最优构型,其结果可以进一步应用到活塞式加热气缸最大功率输出的最优构型和给定输出功率时的最大输出功的最优构型研究中,以及内燃机和外燃机的运行优化中。在此基础上,本节将在给定循环周期 t_m 和给定泵入热流率 $f(t)$ 的条件下,以循环输出功最大为优化目标,进一步研究辐射传热定律下外燃机运行过程的优化问题。

根据文献[6,14],外燃机循环分为完全循环和半循环。假设外燃机在某一时刻 t_i 开始完全循环,工质的体积和温度都将随时间发生周期性变化,所以在时间 $t=t_i+t_m$ 时, $V(t)$ 和 $E(t)$ 都将回复其初始值, $F(t)$ 也应该是周期性函数。故当 $t=t_i+t_m$ 时,式(4)右端的指数部分必为零,可得:

$$\int_{t_i}^{t_i+t_m}\frac{F(t)-U[E(t)/C_V]^4}{E(t)}\mathrm{d}t=0 \tag{6}$$

联立式(3)和式(6),通过数值求解的方法确定 $E(t_i)$。由于增加了 $E(t_i)=E(t_i+t_m)$ 约束,减少了自变量数,故而最优运行过程中的绝热过程不再需要。

在外燃机运行的初始过程中,由于工质温度等于热槽温度 T_{ex},因此在达到稳态初始温度($E(t_i)/C_V$)之前,还需要若干循环来提高工质温度。由于这一系列循环只满足 $V(t_i)=V(t_i+t_m)$,而并不满足 $E(t_i)=E(t_i+t_m)$,所以称之为半循环。半循环由初始绝热过程、中间 $E-L$ 的弧部分和末态绝热过程 3 级组成。在经过一系列半循环之后,工质温度达到稳态初始温度($E(t_i)/C_V$),即工质内能达到 $E(t_i)$ 时,外燃机进入稳态,开始完全循环,初始和末态绝热过程消失。

要确定最优半循环,首先要求出初始绝热过程终点时刻工质内能 $E'(0)$。在文献[6,14]中,由于可以直接求得 $E(t)$ 的解析式,因此令 $\mathrm{d}W/\mathrm{d}E'(0)=0$ 可得初始绝热过程终点 $E'(0)$。辐射传热定律下,由于式(3)是高次方程,无法直接求解得到 $E(0)$ 的解析式,不能通过 $\mathrm{d}W/\mathrm{d}E'(0)=0$ 确定最优半循环初始绝热过程终点 $E'(0)$ 的值。本研究通过

数值求解的方法,利用穷举法,确定半循环初始绝热过程终点 $E'(0)$ 的值。当 $E(t_i)$ 和 $E'(0)$ 确定后,利用式(3)和式(4)可以确定外燃机的最优完全循环和半循环。

对式(1)积分,可得外燃机循环的最大循环功为:

$$W=\int_{t_i}^{t_i+t_m}\cdot F(t)\,\mathrm{d}t+E(t_i)-E(t_i+t_m)-\frac{U}{C_V^n}\int_{t_i}^{t_i+t_m}\cdot E^3(t)\,\mathrm{d}t \tag{7}$$

外燃机循环的效率为:

$$\eta=W/E_p \tag{8}$$

式中: $E_p=\int_0^{t_m}f(t)\,\mathrm{d}t$—泵入系统的总能量。在给定 $f(t)$、T_{ex}、t_m 的条件下,可知最大循环功过程对应最大功率过程和最大效率过程。

3　数值算例

取外燃机气缸膨胀气体的初始体积与末态体积相等,且 $V(0)=V_m=1\times10^{-3}\ \mathrm{m}^3$,理想气体初始内能 $E(0)=3\ 780\ \mathrm{J}$,摩尔热容 $C_V=3R/2$,热槽温度 $T_{ex}=300\ \mathrm{K}$,循环时间 $t_m=2\ \mathrm{s}$,给定泵入热流率 $f(t)=A_f[\sin(\omega t)]^{60}$,其中 $A_f=204\ 722\ \mathrm{J/s}$,$\omega=2\pi/4\ \mathrm{rad/s}$。

表 1　辐射传热定律时 U 变化时各对应值

Tab. 1 Various corresponding values changed with U under the radiation heat transfer law

情形	热导率 U/W·K^{-4}	3.0×10^{-7}	4.0×10^{-7}	5.0×10^{-7}
完全循环	循环初始内能 $E(t_i)$/J	5 407.02	5 143.08	4 960.58
	最优压缩比 γ	49.92	62.83	75.58
	最大循环功/W·J^{-1}	7 838.4	7 597.3	7 376.7
	效率 η	0.1866	0.1809	0.1756
半循环	绝热过程末态内能 $E'(0)$/J	5 232.85	5 015.49	4 861.54
	最优压缩比 γ	68.55	82.60	96.22
	最大循环功/W·J^{-1}	8 677.7	8 231.3	7 879.4
	效率 η	0.2066	0.1960	0.1876

表 1 给出了辐射传热定律时最优完全循环和最优半循环热导率 U 变化时各状态量所对应的值。由表 1 可知,热导率增加,工质对热槽的循环放热量随之增加,外燃机完全循环和半循环的最大循环输出功均减小,因此相应的循环效率减小。与最优完全循环相比,最优半循环的压缩比、循环功和效率较大。这是因为在优化过程中,半循环只满足 $V(t_i)=V(t_i+t_m)$,而并不满足 $E(t_i)=E(t_i+t_m)$,这意味着与完全循环相比,半循环优化的约束条件减少了一个,因此可以得到比最优完全循环更好的优化结果。

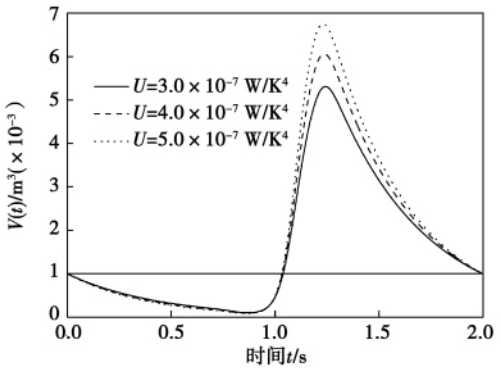

图 2　辐射传热定律时最优完全循环工质体积的时间变化关系

Fig. 2 Optimal full-cycle under the radiation heat transfer law

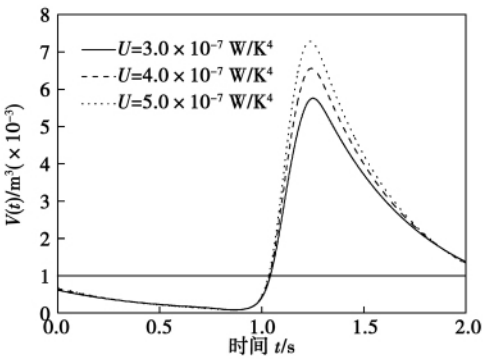

图 3　辐射传热定律时最优半循环工质体积的时间变化关系

Fig. 3 Optimal semi-cycle under the radiation heat transfer law

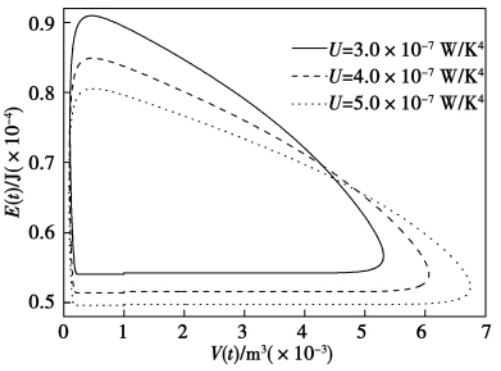

图 4　辐射传热定律时最优完全循环的循环图

Fig. 4 Circulating drawing of the optimal full-cycle under the radiation heat transfer law

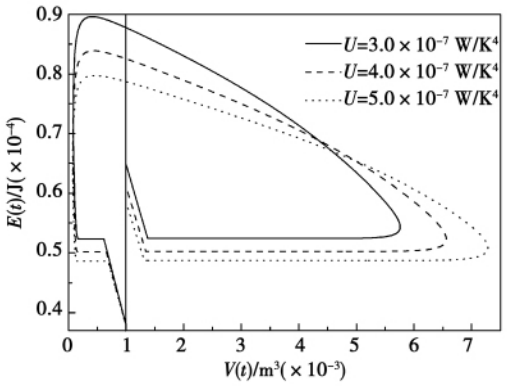

图 5 辐射传热定律时最优半循环的循环图

Fig. 5 Circulating drawing of the optimal semi-cycle under the radiation heat transfer law

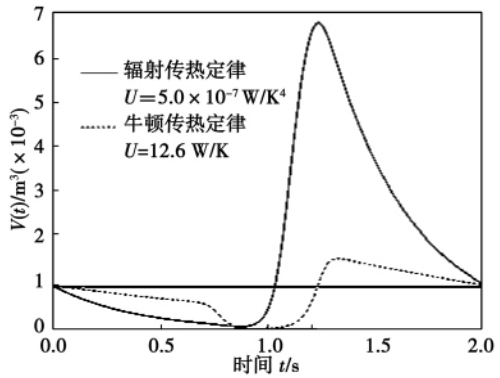

图 6 辐射和牛顿传热定律下最优完全循环工质体积的时间变化关系

Fig. 6 Relationship between the volume of the optimal full-cycle working medium and time under the radiation and Newton heat transfer law

图 2 和图 3 分别为辐射传热定律时最优完全循环和最优半循环工质体积的时间变化关系，图 4 和图 5 分别为辐射传热定律时最优完全循环和最优半循环的循环图。由图 2 可知，最优完全循环时，工质体积随时间的变化规律类似于正弦曲线，并且完全循环是由初期的压缩过程、中间的膨胀做功过程和末态的压缩过程等 3 部分组成。初始和末态压缩过程持续时间较长，而中间的膨胀做功过程相对较短（大约 0.5 s 内），工质体积急剧膨胀，完成对外做功。由图 2 还可以看出，热导率增加，膨胀过程的最大体积随之增加。这是因为热导率增加，工质向热槽的循环放热量增加，循环做功能力减小，必须通过增加做功过程的最大体积来弥补做功能力的减小。由图 3 可知，半循环由初始的绝热压缩过程、中间的 $E-L$ 弧部分和末态绝热膨胀过程等 3 部分组成。在中间的 $E-L$ 弧部分与最优完全循环相似，工质体积随时间的变化规律也是类似于正弦曲线，并且也是由初期的压缩过程、中间的膨胀做功过程和末态的压缩过程等 3 部分组成。热导率增加，$E-L$ 弧部分膨胀过程的最大体积随之增加。从图 4 中可知，热导率增加，工质对热槽放热随之增加，因此工质的循环最大内能减小。半循环过程只满足 $V(t_i)=V(t_i+t_m)$，而并不满足 $E(t_i)=E(t_i+t_m)$，每一个循环结束，缸内工质温度都有提高，当缸内工质温度达到稳态初始温度（$E(t_i)/C_V$）时，工质进入完全循环，工质温度与内能同时周期性变化。

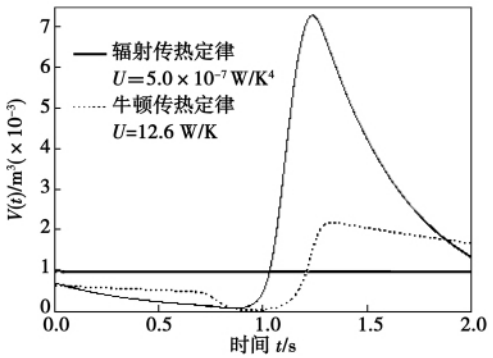

图 7 辐射和牛顿传热定律下最优半循环工质体积的时间变化关系

Fig. 7 Relationship between the volume of the optimal semi-cycle working medium and time under the radiation and Newton heat transfer law

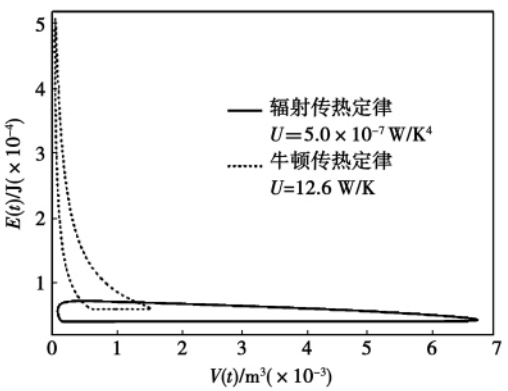

图 8 辐射和牛顿传热定律下最优完全循环的循环图

Fig. 8 Circulating drawing of the optimal full-cycle under the radiation and Newton heat transfer law

图 6 和图 7 分别为辐射和牛顿传热定律下最优完全循环和最优半循环工质体积的时间变化关系，图 8 和图 9 分别为辐射和牛顿传热定律下最优完全循环和最优半循环的循环图。由图 6 ~ 图 9 可知，虽然

不同传热定律下完全循环和半循环的 $E-L$ 弧部分，工质体积随时间的变化规律均类似于正弦曲线，并且均由 3 部分组成，但由于传热定律不同，工质体积随时间的变化曲线却完全不同，主要区别表现在 3 个方面：(1) 对于最优完全循环和最优半循环的 $E-L$ 弧部分，3 部分的时间分配完全不同，这意味着工质的循环最小和最大体积对应的时间不同；(2) 工质的循环最小和最大体积以及最大内能完全不同；(3) 对于半循环，初始绝热压缩过程的末态工质体积和内能完全不同，这直接导致最优半循环的 $E-L$ 弧部分工质体积的时间变化关系不相同。

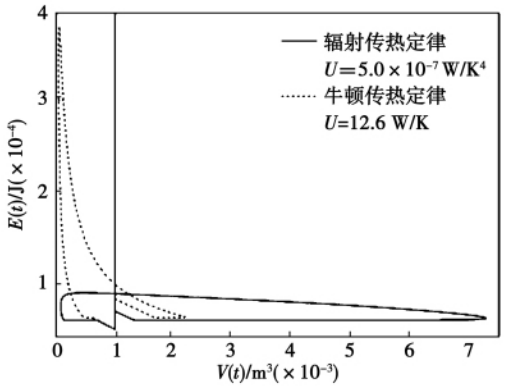

图 9　辐射和牛顿传热定律下最优半循环的循环图

Fig. 9 Circulating drawing of the optimal semi-cycle under the radiation and Newton heat transfer law

4　结　论

以活塞式外燃机为研究对象，考虑工质与外热槽间传热服从辐射传热定律 [$q\propto\triangle(T^4)$]，以循环输出功最大为优化目标对外燃机进行了优化。给出了辐射传热定律时的数值算例，并与牛顿传热定律下的结果进行了比较。结果表明，辐射传热定律下，热导率增加，由于工质对热槽的循环放热量随之增加，外燃机完全循环和半循环的最大循环输出功均减小，因此相应的循环效率减小。与最优完全循环相比，最优半循环的压缩比、循环功和效率较大。通过比较辐射和牛顿传热定律下结果可知，虽然不同传热定律下最优完全循环和最优半循环的欧拉-拉格朗日($E-L$)弧部分，工质体积随时间的变化规律均类似于正弦曲线，并且均由 3 部分组成，但不同传热定律时工质体积随时间的变化曲线和循环图是不相同的，主要区别表现在 3 个方面：(1) 对于最优完全循环和最优半循环的 $E-L$ 弧部分，3 部分的时间分配完全不同，这意味着工质的循环最小和最大体积对应的时间不同；(2) 工质的循环最小和最大体积以及最大内能完全不同；(3) 对于半循环，初始绝热压缩过程的末态工质体积和内能完全不同，这直接导致最优半循环的 $E-L$ 弧部分工质体积的时间变化关系不相同。在活塞式外燃机模型中引入了辐射传热定律，从牛顿传热定律 [$q\propto\triangle T$] 到辐射传热定律 [$q\propto\triangle(T^4)$] 的研究，丰富了有限时间热力学理论，使其更加系统和完善。

参考文献：

[1] CHEN L, WU C, SUN F. Finite time thermodynamic optimization or entropy generation minimization of energy systems [J]. J Non-Equilib. Thermodyn, 1999, 24(4): 327-359.

[2] CHEN L, SUN F. Advances in finite time thermodynamics: analysis and optimization [M]. New York: Nova Science Publishers, 2004.

[3] 陈林根. 不可逆过程和循环的有限时间热力学分析 [M]. 北京：高等教育出版社, 2005.
CHEN Li-gen. Finite-time Thermodynamic analysis of irreversible processes and cycles [M]. Beijing: Higher Education Press, 2005..

[4] BAND Y B, KAFRI O, SALAMON P. Maximum work production from a heated gas in a cylinder with piston [J]. Chem. Phys. Lett, 1980, 72(1): 127-130.

[5] BAND Y B, KAFRI O, SALAMON P. Finite time thermodynamics: optimal expansion of a heated working fluid [J]. J Appl Phys, 1982, 53(1): 8-28.

[6] BAND Y B, KAFRI O, SALAMON P. Optimization of a model external combustion engine [J]. J Appl Phys, 1982, 53(1): 29-33.

[7] SALAMON P, BAND Y B, KAFRI O. Maximum power from a cycling working fluid [J]. J Appl Phys, 1982, 53(1): 197-202.

[8] AIZENBUD B M, BAND Y B. Power considerations in the operation of a piston fitted inside a cylinder containing a dynamically heated working fluid [J]. J Appl Phys, 1981, 52(6): 3742-3744.

[9] AIZENBUD B M, BAND Y B, KAFRI O. Optimization of a model internal combustion engine [J]. J Appl Phys, 1982, 53(3): 1277-1282.

[10] CHEN L, SUN F, WU C. Optimal expansion of a heated working fluid with phenomenological heat transfer [J]. Energy Convers Mgmt, 1998, 39(3/4): 149-156.

[11] CHEN L, SONG H, SUN F, et al. Optimal expansion of a heated working fluid with convective-radiative heat transfer law [J]. Int J Ambient Energy, in press.

[12] SONG H, CHEN L, SUN F. Optimal expansion of a heated working fluid for maximum work output with generalized radiative heat transfer law [J]. J Appl Phys, 2007, 102(9): 094901.

[13] 马　康，陈林根，孙丰瑞. 广义辐射传热定律时加热气体最优膨胀的一种新解法 [J]. 机械工程学报, 2010, 46(6): 149-157.
MA Kang, CHEN Lin-gen, SUN Feng-rui. A new method for seeking solutions to the optimal expansion of heated gas under the generalized radiation heat transfer law [J]. Journal of Mechanical Engineering, 2010, 46(6): 149-157.

[14] SONG H, CHEN L, SUN F. Optimization of a model external combustion engine with linear phenomenological heat transfer law [J]. J Energy Inst, 2009, 82(3): 180-183.

[15] CHEN L, SONG H, SUN F, WU C. Optimization of a model internal combustion engine with linear phenomenological heat transfer law [J]. Int J Ambient Energy, 2010, 31(1): 13-22.

Experimentally studied were the partial load characteristics of a gas-engine-driven heat pump unit and mainly analyzed was the law governing the influence of the end water flow rate and rotating speed on the heat production performance of the unit. It has been found that the load of the condenser, total waste heat, performance coefficient and primary energy source utilization rate will all increase with an increase of the end water flow rate. When the end water flow rate increases from 1.8 m^3/h to 3.6 m^3/h, the performance coefficient and primary energy source utilization rate will increase by 11.6% and 19.5% respectively. The load of the condenser and the total waste heat will increase with an increase of the rotating speed of the engine and the performance coefficient and the primary energy source utilization rate, however, will decrease by 40% and 9.8% respectively when the rotating speed of the engine increases from 1300 r/min to 2000 r/min. The gas-engine-driven heat pump unit boasts good partial load characteristics at various end water flow rates and rotating speeds of the gas-engine. **Key words:** gas-engine-driven heat pump, heat production operating condition, variable end water flow rate, variable speed, partial load

纳秒脉冲等离子体气动激励控制平板附面层的研究 = Study of the Boundary Layer on a Plate Aerodynamically Excited and Controlled by Using Nanosecond Pulse Plasma [刊,汉] YUE Tai-peng, LI Ying-hong, SUN Dong, CUI Wei (Engineering College, Air Force Engineering University, Xi'an, China, Post Code: 710038) //Journal of Engineering for Thermal Energy & Power. - 2011, 26(5). -528 ~ 532

To study the working mechanism of the boundary layer on a plate aerodynamically excited and controlled by using nanosecond pulse plasma and the law governing its change under different parameters, the speed of air flow aerodynamically excited and controlled by using the nanosecond pulse plasma was measured by utilizing a self-developed velocity measurement system. The measurement results show that under different combined excitation modes, the aerodynamic excitation effectiveness by using the plasma is varied and that produced by using the medium barrier discharge is regarded as the best. That achieved by using the nanosecond plasma to excite and induce the air to accelerate will be enhanced with an increase of the excitation voltage. Its effectiveness played on a low speed air flow is better than that on a high speed air flow. The jet flow direction aerodynamically excited and induced by using the nanosecond pulse plasma forms a certain angle with the wall surface. Along the downstream direction, the air flow acceleration effectiveness aerodynamically excited and induced by using the plasma is weakened obviously. **Key words:** aerodynamic excitation by using plasma, boundary layer, induction, excitation combination, medium barrier discharge

辐射传热定律下外燃机最大输出功优化 = Optimization of the Maximum Power Output of an External Combustion Engine Under the Law of Radiation-based Heat Conduction [刊,汉] MA Kang, CHEN Lin-gen, SUN Feng-rui (Postgraduate School, Naval Engineering University, Wuhan, China, Post Code: 430033) // Journal of Engineering for Thermal Energy & Power. -2011, 26(5). -533 ~ 537

With a piston-type external combustion engine serving as an object of study, optimized was an external combustion

engine with the maximal power output of the cycle serving as the optimization target and the heat conduction between the working medium and the external heat channel abiding by the law of radiation-based heat conduction [$q \propto \Delta(T^4)$]. A numerical calculation case was given under the law of radiation-based heat conduction and compared with the results obtained under the Newton's heat law. The results of the numerical calculation case show that with an increase of the heat conductivity, the power output and efficiency of the optimal full and semi cycle will decrease. Compared with the full cycle, the compression ratio, power output and efficiency of the optimal semi-cycle are relatively big. Although the Euler-Lagrange ($E-L$) arc sections and the curves showing the change of the volume of the working medium with time are all similar to sine curves and composed of three sections under both heat conduction laws, the curves showing the change of the volume of the working medium under different heat conduction laws are not a same one. **Key words:** finite-time thermodynamics, law of radiation-based heat conduction, maximal power output, external combustion engine

气液两相流流型图像信息熵递归特性分析 = Analysis of the Image Information Entropy Recurrence Characteristics of a Gas-liquid Two-phase Flow Pattern [刊,汉] HONG Wen-peng, LIU Yan, ZHOU Yun-long (College of Energy Source and Power Engineering, Northeast University of Electric Power, Jilin, China, Post Code: 132012) // Journal of Engineering for Thermal Energy & Power. - 2011, 26(5). -538 ~542

By using a high speed video camera, acquired were the flow images of various flow patterns of two kinds of tube bundle in 10 rows and 4 columns with a pitch of 1.3 and 1.8 respectively. In the light of the typical flow images in three types, namely bubble - shaped flow, intermittent flow and mist flow, the information entropy sequence of the various flow pattern images was extracted and the dynamic characteristics of various flow patterns of the gas-liquid two-phase flow and the entropy sequence of the transit flow patterns were studied by using the recurrence analytic method. The research results show that the recurrence structures of the entropy sequences of different flow pattern images are different. The recurrence chart of the information entropy sequence of the bubble-shaped flow images is of a dot-shaped structure, that of the intermittent flow images is of a dot-block-shaped structure while that of the mist flow is of a clearest diagonal structure. The recurrence structures of the entropy sequences of transit flow pattern images can clearly show the evolvement of the transition process of the flow patterns. The recurrence structure chart of information entropy sequence can reflect relatively well the evolvement mechanism of the flow patterns and the recurrence characteristic variable is susceptible to the change of converted flow speed, thus providing a relatively effective method for studying the mechanism governing the flow patterns of gas-liquid two-phase flow. **Key words:** gas-liquid two-phase flow, tube bundle, flow pattern, information entropy, recurrence chart

带肋矩形直通道内的冷却空气换热特性研究 = Study of the Heat Exchange Characteristics of the Cooling Air Inside a Straight Ribbed Rectangular Channel [刊,汉] LIU Rui, SHUI Lin-qi, WANG Xin-jun, BAI Xiao-wei (Turbo-machinery Research Institute, Xi'an Jiaotong University, Xi'an, China, Post Code: 710049) // Journal of Engineering for Thermal Energy & Power. - 2011, 26(5). -543 ~546